Presented at 3rd International Symposium on Environmental Management, SEM – Towards Sustainable Technologies (SEM2011) at University of Zagreb, Faculty of Chemical Engineering and Technology, 26–28 September, 2011, Zagreb, Croatia

Sol-gel Derived Mixed Metal Oxide Sorbents for High Temperature Gas Desulfurization

V. Mandić,[a] T. Očko,[b] G. Matijašić,[a] and S. Kurajica[a]
[a]Faculty of Chemical Engineering and Technology, University of Zagreb, Marulićev trg 19, Zagreb, Croatia
[b]Vetropack Straža d.d. Hum na Sutli, Croatia

Original scientific paper
Received: September 18, 2012
Accepted: February 5, 2013

High temperature gas desulfurization (HTGD) is the main process for hydrogen sulphide removal from hot gases. Currently leading regenerable desulfurization sorbents are based on ZnO–TiO_2 system. This work presents structural and textural modifications of ZnO–TiO_2 based sorbents by Al_2O_3 addition in order to ensure high temperature mechanical support. Sorbents with composition $Zn_{(2-x)}Al_{2x}Ti_{(1-x)}O_4$ (x = 0, 0.25, 0.5, 0.75, 1) were prepared by sol-gel process followed by thermal treatment. Nanocrystalline powders were produced at moderate sintering conditions (500 °C, 2 h). Depending on the initial ZnO:TiO_2:Al_2O_3 molar ratio, zincite (ZnO), brookite (TiO_2) as well as gahnite ($ZnAl_2O_4$) solid solution were formed. Al_2O_3 induced textural modifications, rising specific surface area from 34 to 90 $m^2\ g^{-1}$. The sorbent sulphidation performance was tested using newly developed procedure comprising batch sulphidation process. Sorbent with composition $Zn_{1.75}Al_{0.5}Ti_{0.75}O_4$ was found to possess the highest sulphidation reactivity, i.e. sulphur removal efficiency.

Key words:
HTGD, desulfurization, sorbent, ZnO–Al_2O_3–TiO_2

Introduction

Integrated gasification combined cycle (IGCC) is one of the most promising processes for producing electrical energy from coal due to the noticeable improvement in thermal efficiency that it can provide. This advanced power-generating system involves the direct contact of hot coal-derived gases with turbine blades. In order to ensure high environmental requirements, as well as corrosion and abrasion protection of the turbines and related equipment, precleaning of the coal gas from pollutants, especially hydrogen sulphide, H_2S, is necessary. Economic as well as environmental aspects for advanced power-generating systems mandate the high temperature gas desulfurization (HTGD) as the main process for the removal of the most abundant sulphur-containing compound in coal gas, hydrogen sulphide, which can react readily with the oxides of alkali earth and transition metals.[1]

The development of metal oxide materials as durable, chemically, mechanically, and thermally stable regenarable sorbents, capable of supporting multiple desulfurization-regeneration cycles, has been the goal of several studies.[2–5] In a vast number of metal oxides proposed, zinc-oxide based sorbents are recognized as those with the best cost-benefit ratio and are proven HTGD sorbents for removal of hydrogen sulphide.[6–8]

Despite the fact that zinc-oxide ensures efficient reduction of hydrogen sulphide content to the ppm level, it is unable to provide a long-term stable desulfurization-regeneration process. Namely, desulfurization conditions promote reduction of Zn^{2+} to Zn, and due to harsh temperature process conditions, the zinc evaporate from the sorbent.[9] Another weakness of zinc oxide are its insufficient mechanical properties yielding wearing during fluidization in the course of the sulphidation-regeneration process.[10,11]

In order to surpass these disadvantages, a combination of zinc oxide with other compounds was

*Corresponding author: Vilko Mandić, e-mail: vmandic@fkit.hr

investigated.[12–14] It was observed that combination of Zn-based sorbents with other metal oxide compounds can greatly improve the performance of mixed-metal sorbents in several aspects, especially the ones pointed out as disputable. Enhanced performance can be expected in terms of greater sulfur removal efficiency, in decrease of the Zn^{2+} reduction and in the suppression of sulfate formation, all with retained mechanical strength, structure of micropores, and overall reactivity and stability of sorbent particles. TiO_2 and Al_2O_3 were emphasized as most useful for combining. Combination with compounds like titanium oxide can provide thermal stability of the sorbent, i.e. prevent evaporation of the zinc.[15] On the other hand, by combination with Al_2O_3, which is proven as a high-temperature stable and durable material, mechanical wearing and attrition of the sorbent can be minimized. Also the high temperature sintering process should be postponed, influencing the pore structure which should lead to an increase in specific surface. By the enlarged interaction interface, a better desulfurization efficiency should be noticed.[10,11]

The ability to provide an efficient sorbent should not only be focused on optimizing the chemical composition but also a proficient production technique. A vast number of sorbents are prepared by high temperature techniques which could annul the benefits achieved by chemical composition.[6,16] Therefore a technique which offers the possibility of achieving sorbent synthesis at lower temperatures, the sol-gel technique, should be applied.[17]

In this work several compositions of the $ZnO–Al_2O_3–TiO_2$ based sorbent were synthesized by means of sol-gel process and investigated. Yielded sorbent performance was tested by newly developed high-temperature and high-pressure sulphidation process in batch reactor.

Experimental

Materials used to prepare precursor gels were Aluminum sec butoxide (Asb, $Al(O^sBu)_3$, 97 %, Acros organics, Belgium), Titanium n-butoxide (Tnb, $Ti(O^nBu)_4$, 98 %, Alfa Aesar, Germany), Zinc nitrate hexahydrate ($Zn(NO_3) \times {}_26H_2O$, 98 %, Riedel-de Haën, Germany). Ethyl acetoacetate (Eaa, $C_6H_{10}O_3$, 99 %, Fluka, Germany) was used as a complexing agent while Isopropyl alcohol (C_3H_7OH, 99 %, Carlo Erba Reagents, Italy) was used as a solvent. All chemicals were used as received.

The appropriate amounts of Asb and Tnb were dissolved in Eaa and isopropyl alcohol solution independently; also zinc nitrate hexahydrate was dissolved in isopropyl alcohol. The molar ratio of Asb and Tnb to Eaa was held 1/1 as it was previously experimentally proven optimal.[18] The mixtures were stirred 30 minutes. The Tnb solution was then added dropwise to Asb solution and stirred for an additional 30 minutes. After that the Zn nitrate solution was added in the same manner, the mixture was stirred for 24 hours at room temperature during which the gelation occurred. The obtained samples were subsequently ground to fine powder and stored. For the experiment five gels were prepared with compositions 0.500 ZnO × 0.500 Al_2O_3, 0.556 ZnO × 0.333 Al_2O_3 × 0.111 TiO_2, 0.600 ZnO × 0.200 Al_2O_3 × 0.200 TiO_2, 0.636 ZnO × 0.091 Al_2O_3 × 0.273 TiO_2 and 0.667 ZnO × 0.333 TiO_2, corresponding to the ternary diagram intersections as shown in Fig. 1, and denoted accordingly.

IR spectra of the samples were acquired using the Fourier transform infrared spectrometer Bruker Vertex 70 in ATR (attenuated total reflectance) mode. The samples were pressed on a diamond and the absorbance data were collected between 400 and 4000 cm^{-1} with spectral resolution of 1 cm^{-1} and 64 scans.

The crystal phases were identified by powder X-ray diffraction (XRD) using Shimadzu diffractometer XRD 6000 with CuKα radiation. Data were collected between 5 and 70° 2θ in a step scan mode with steps of 0.02° and scan speed of 2° 2θ min^{-1}.

The thermal behavior of powder precursor was characterized with Differential Thermal Analysis (DTA) and Thermo-Gravimetric Analysis (TGA) using simultaneous DTA/TGA analyzer Netzsch STA 409. For the thermal analysis approximately 50 mg of material were placed in Pt crucibles and heated at a rate of 10 °C min^{-1} to 1000 °C in a syn-

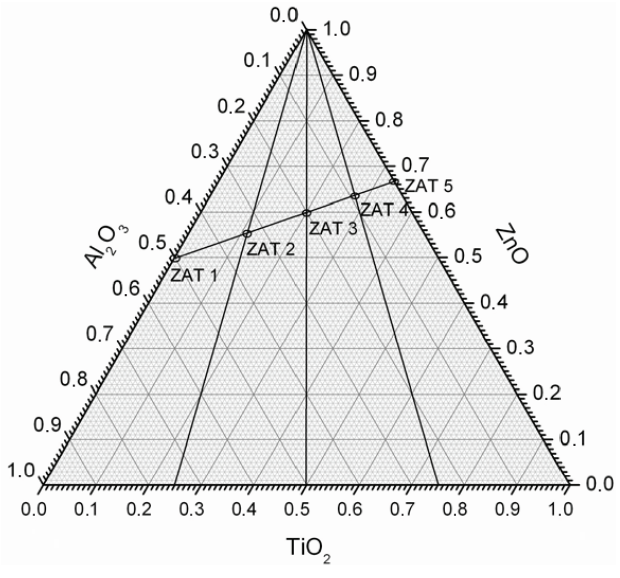

Fig. 1 – *Samples molar composition and notation*

thetic air flow of 30 cm^3 min^{-1}, α-alumina was used as a reference.

Specific surface area of powders was determined by a Brunauer–Emmet–Teller (BET) N_2 gas adsorption-desorption isotherm obtained at 77 K on a Micromeritics ASAP 2000 equipment. Sample was previously degassed at 400 °C under a dynamic vacuum of $1.3 \cdot 10^{-2}$ Pa.

Sulphidation process was performed in a batch autoclave. Approximately 250 mg of all samples ZAT 1 – 5 and reference ZnO sample were placed in separate crucibles in the reactor. Separately, FeS grains and 10 % HCl were prepared in order to produce H_2S. Reactor was heated at 200 °C for 2 hours.

The extents of sulphidation of sorbents in the autoclave assembly were monitored as weight changes during oxidation, i.e. regeneration process, by Thermo-Gravimetric Analysis (TGA) using Perkin Elmer TGS-2. A small amount of sulphidated sorbent was placed in Pt crucible and heated at a rate of 10 °C min^{-1} to 1000 °C in a synthetic air flow. The conversion of the sulphidation process was calculated from the partial mass loss in the course of the oxidation process:

$$ZnS + 3/2\ O_2 \rightarrow ZnO + SO_2$$

Conversion was determined from the appropriate section of the thermogravimetric curve using equations:

$$\Delta m_{\max} = \frac{M_{ZnS} - M_{ZnO}}{M_{ZnS}} \cdot 100\,\%$$

$$conversion = \frac{\Delta m_{reg}}{\Delta m_{\max}} \cdot 100\,\%$$

Results and discussion

From the FTIR investigation of the gels, information about the chelation process can be obtained. Infrared spectra of the samples ZAT 1 – ZAT 5 dried gels are presented in Fig. 2. The FTIR spectra of Eaa-based chelates are assigned as described in literature.[19] Majority of alkoxides react readily when exposed to water (even air humidity). The hydrolysis of some alkoxides, among which are Asb and Tnb, occur rapidly. The role of Eaa, which was added to the system, is to stabilize the rate of alkoxide hydrolysis by forming a chelate with alkoxide. Namely, ß-ketoesters like Eaa resonate between keto and enol form (keto-enol tautomerism), in which the keto form is favored in pure Eaa, while upon forming chelate with alkoxide the enol form dominates. Monitoring of the keto-enol equilibrium enables the insight in the processes of hydrolysis and condensation, i.e. in the sol-gel process.

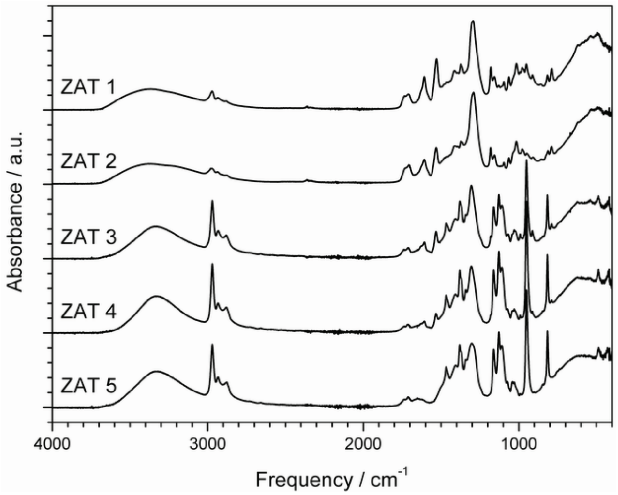

Fig. 2 – *IR spectra of samples ZAT 1 – 5*

In the IR spectra of all dried gels several characteristic bands occur which could be assigned to Eaa. Both keto and enol form of Eaa yield with characteristic absorption bands in region 2980–2850 cm^{-1} originating from C–H stretching vibrations. Band at 2980 cm^{-1} results from the asymmetrical stretching mode in which two C-H bonds of the methyl group are extending, while the third one is contracting (ν_{as} CH_3). Band at 2870 cm^{-1} arises from symmetrical stretching (ν_s CH_3) in which all three C–H bonds extend and contract in phase. The asymmetrical stretching (ν_{as} CH_2) and symmetrical stretching (ν_s CH_2) occur at 2940 and 2850 cm^{-1}, respectively. Also, bands at 1475 cm^{-1} (as asymmetrical bending vibration involves out-of-phase bending of the C–H bonds, δ_{as} CH_3) and 1369 cm^{-1} (as symmetrical bending vibration involves in phase bending of the C–H bonds, δ_s CH_3) were noticed. The CH_2 scissoring band in the spectrum occurs at 1470 cm^{-1}. The absorption frequencies from O–C–C stretching, –C–C–O stretching and C–C stretching occur at 1040 cm^{-1}, 1155 cm^{-1} and 1317 cm^{-1}, respectively.

Band characteristic exclusively for the keto form of Eaa occurs at 1753–1718 cm^{-1} due to the C=O stretching vibration of two carbonyl groups. Instead of bands of the keto form, in the spectrum of enolic form characteristic bands are observed at 1650 cm^{-1} due to hydrogen bonding between the ester C=O and the enolic hydroxyl group, as well as absorption frequencies of the alkene bond in conjugation with a carbonyl group at 1630 cm^{-1}. Eaa in chelate shows characteristic absorption bands at ~1610 cm^{-1} due to a C–O in enolic form bonded to

Al, as well as absorption band at ~1525 cm^{-1} due to a C-C vibration of six membered ring of the complex. The major absorption bands due to a NO_3^- are located at 1305, 1445 and 1630 cm^{-1}, mostly overlapped with Eaa bands.

FTIR spectra presented in Fig. 2 confirm that Eaa, in all samples, i.e. for all Eaa/Asb/Tnb ratios, reacts with alkoxides and forms chelate. As can be seen, although the dominance of the enol form was observed, during the hydrolysis and polycondensation processes in the course of the synthesis, a part of Eaa in the keto form was entrapped and remained even in dried samples.

In frequencies 400–600 cm^{-1} weak bands resembling $[ZnO_6]$ and $[ZnO_4]$ polyhedra are observed.[20] At frequencies from 550–650 cm^{-1} bands of $[TiO_6]$ are expected.[20] Frequencies characteristic for Al-O-Al linkages[21] occur at ~700 cm^{-1}. In IR spectra of the raw gels most of the bands characteristic for M-O bonds are highly overlapped, as bands related to the organic component predominate and thus are difficult to observe.

The thermal behavior of all dried gels is characterized by multistep weight loss in the temperature range of 100–450 °C as shown by DTGA measurement in Fig. 3. In the higher temperature region the weight loss is constant at approximately 55 % mass loss for all samples (TGA scan, not shown in Fig. 3). DTA curves of all samples consist of a series of endothermic and exothermic effects with various intensity and mutual superposition (not shown in Fig. 3) and correspond well to DTGA data in Fig. 3. In the temperature range below 200 °C observed phenomena are related to the subsequent releases of adsorbed water. Chemisorbed water is removed also up to the temperature of 300°C. Furthermore solvent degradation follows. The occurrence temperature and intensity of these processes, and especially the following ones representing

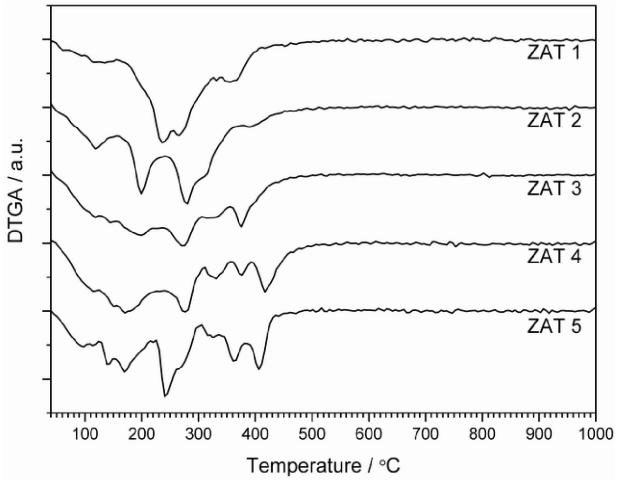

Fig. 3 – *DTGA scans of samples ZAT 1 – 5*

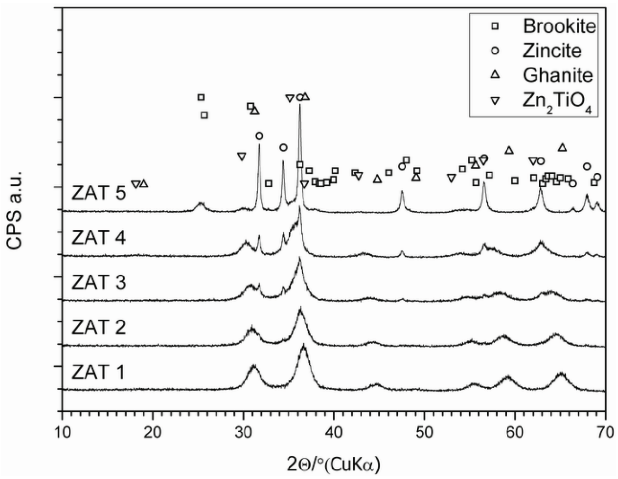

Fig. 4 – *Diffractograms of samples ZAT 1 – 5 fired at 500 °C for 2 hours*

chemical transformations are related to distinct chemical species present in the gels. Due to gradual change of composition of the gels it is possible to observe similarities in thermal effects. However, due to high level of mutual superposition if is difficult to assign specific transformations. Despite, some processes accompanied with high mass loss can be observed overall in samples, such as the nitrates decomposition process, occurring at about 250 °C.[22] At temperatures above 300 °C, the effects occurring can be related to crystallization processes in the system. A series of DTGA peaks centered at ~400 °C with increasing intensity in samples containing more Zn can be attributed to the decomposition of $Zn(OH)_2$ (crystallization of ZnO). Having in mind the composition of the gels, several crystal phases may occur; however, to provide exact assignation of DTA effects, structural investigations should have been performed at various temperatures. Instead, crystal composition was monitored after thermal treatment at the temperature of 500 °C and discussed in XRD section.

Samples were fired at temperature as low as 500 °C for 2 hours in order to preserve high specific surface area, as the temperature increase would promote sintering and therefore cause the reduction of the specific surface area. All ZAT samples fired at 500 °C were subjected to XRD analysis in order to determine phases present in the studied system (Fig. 4). All scans exhibit crystalline phases. Chemical composition of the sample ZAT 1 was targeted to fit gahnite which was confirmed using XRD. ZAT 5 should fit to Zn_2TiO_4, which was also confirmed. Samples ZAT 2, 3 and 4 resemble the composition and phases chemically between the two mentioned (zinc alumotitanate solid solutions). In samples ZAT 2 – 5 zincite, ZnO, has been evidenced, also with increasing intensities resembling

Zn content increase. In sample ZAT 5 brookite, TiO_2, crystallized.

To facilitate high efficiency of the sorbent, it is essential to provide reaction interface as immense as possible during the whole cycle. The conversion of ZnO to ZnS during the desulfurization process, involves significant volume changes (molar volume +50 %). Small specific surface area would disable or significantly reduce the rate of the conversion process as the gas diffusion resistance would be increased on behalf of the reaction volume increase, especially in the later stage of the reaction. Smaller particles can also ease up the diffusion resistance during the regeneration process of the sorbent samples.[23] To evaluate if the material preparation has been successful in terms of achieving high specific surface area, a series of BET N_2 adsorption-desorption isotherms were measured. The determined specific surface areas are shown in Table 1. Reasonably high S_{BET} have been obtained for all samples. As can be seen, the greater alumina content yields better surface properties, while the complete absence of alumina yields significant decrease of specific surface area. The opposite can be observed for samples with higher ZnO loading. The alumina containing gels yield finer particles.[24] Furthermore, ZnO loading enhances grain growth and promote aggregation with crystallized spinel particles. Both processes result in larger pores and thus smaller specific surface area.[25] It was shown that high surfaces area is necessary for efficient gas removal; however it can also ensure greater mechanical durability of the whole composite. Finer particles ensure mechanical strength necessary for harsh fluidization conditions and also longer lifetime of the sorbent. Namely, repetitive sulphidation-regeneration cycle is accompanied with volume changes which generate strain in the sorbent. Sorbent with limited conversion capabilities (low specific surface area) would not be able to withstand these forces and would have poor lifetime expectancy.

In order to investigate the feasibility of the samples as a regenerable high temperature desulfurization sorbents a whole sulphidation-regeneration cycle (ZnO–ZnS–ZnO) was simulated. Samples were partially converted to ZnS in a simulated sulphidation process involving batch autoclave for H_2S exposure, while thermogravimetric analysis in synthetic air simulated regeneration process. Generally, setup for sulphidation/desulfurization experiment usually consist of feed gas dosing section, equipped with mass flow controller, heated quartz reactor tube, where sulphidation and regeneration occur, and equipment for measurement of the composition of the gas leaving the reactor.[26] The basic flaws of described setup are complexity, the presence of temperature and gas composition gradient and non-uniformity of the gas velocity.[26] In order to develop a simpler and more affordable procedure for testing the potential of prepared sorbents for hot-gas desulfurization process, a new type of sulphidation experiment setup has been designed. The extent of the reaction between prepared sorbents fine particles and H_2S has been studied using teflon-lined stainless steel laboratory autoclave. The autoclave is a closed stainless steel vessel with an internal cup and lid made of teflon. The autoclave can be charged with reagents, and tightly closed. Under external heating, the contents will be raised to high temperatures and pressures. For the purpose of this experiment the autoclave has been modified by adding the internal rack splitting the vessel in two parts as shown in Fig. 5. In lower part a hydrogen sulphide gas has been produced by the reaction of iron sulphide with hydrochloric acid. Holes in rack enabled undisturbed passage of H_2S to upper part where powder samples were placed in small glass crucibles. Under high temperature and pressure hydrogen sulphide reacts with samples forming metal sulphide. To the best of our knowledge, such experimental setup for sulphidation experiment has not been described previously. Unfortunately, although the described procedure is simpler and shows no usual disadvantages of flow reactor,

Table 1 – *BET specific surface of samples ZAT 1 – 5*

Sample	Specific surface area / $m^2\ g^{-1}$
ZAT 1	89.58
ZAT 2	88.98
ZAT 3	79.05
ZAT 4	67.74
ZAT 5	33.58

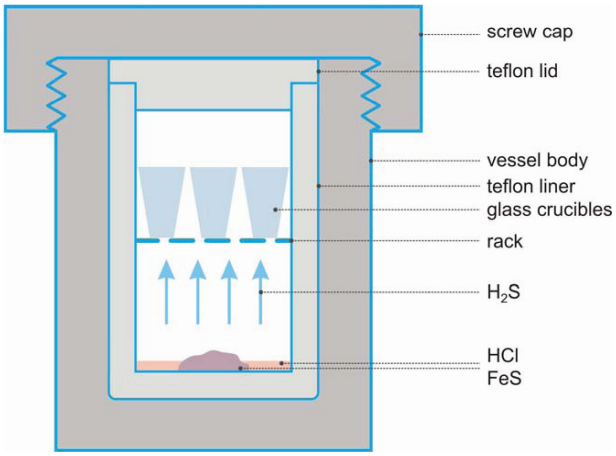

Fig. 5 – *A schematic representation of experimental assembly*

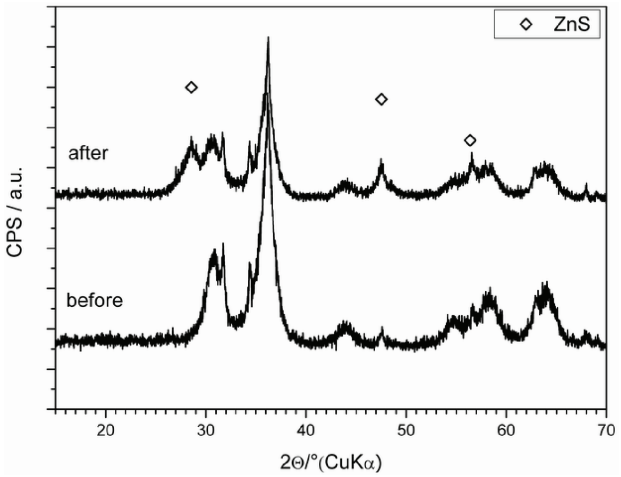

F i g . 6 – *Comparison of diffractograms of sample ZAT 3 before and after sulphidation*

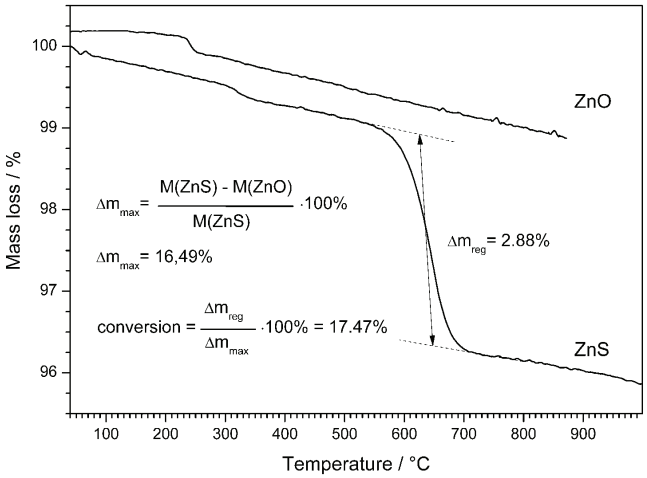

F i g . 7 – *TGA regeneration of sulphidated ZnO reference sample*

it is not flawless. While it is very useful for comparison of powders sulphidation ability, it is not adequate for the kinetic investigation and all experiments involving variations in temperature, due to mutual dependence of temperature and pressure in the vessel. After sulphidation process all samples were structurally analyzed by means of XRD analysis. The diffractograms of sample ZAT 3 before and after sulphidation are shown as example (Fig. 6). All scans generally resemble very well the diffractograms before sulphidation with one major difference; the occurrence of ZnS diffraction lines in all samples in various intensity. At the same time the intensity of zincite and spinel diffraction lines was reduced. Obviously, during the sulphidation process ZnO and spinel solid solution were partially converted to ZnS. In such manner a change of the crystal composition in the samples was established and the reliability of the batch sulphidation method was confirmed. By enabling sufficient conversion to ZnS, the procedure served as a satisfactory method for simulation of conditions that real sorbent would have to go trough in a HTGD process.

The regeneration results enabled the validation of pollutant removal efficiency of samples with different compositions. The amount of ZnS formed during the sulphidation process could be calculated from the mass loss during the regeneration process as shown in Fig. 7. The TGA curve of reference sample (pure zincite) was used to demonstrate the procedure. Assuming that all of the formed ZnS regenerates back to ZnO during the TGA measurement (in synthetic air flow), the calculation of the sulphidation efficiency is enabled only from ratio of molar masses. The regenerated sorbents did not sinter during the regeneration process; moreover no zinc sulfate (which can significantly decrease sorbent sulphide removal efficiency) was formed during the regeneration. For samples ZAT 1 – 5 the results are given in Table 2. As can be seen, sample ZAT 4 (composition $Zn_{1.75}Al_{0.5}Ti_{0.75}O_4$) exhibits the best sulphidation efficiency with conversion of 33.90 %. Such efficiency is in accordance with already reported results. Namely, in the case of Zn-based HTGD sorbents, quite uniform pollutant removal results can be revealed from literature. The conversions in successful sulphidation-regeneration cycle are primarily function of the Zn content and were mostly reported to range from 5–22 %.[16,27,28] Obviously, it is proven that the Zn content provides a main contribution in removal activity. However, as already mentioned, the Zn content has an inverse influence on sulphidation efficiency and mechanical durability. Both aspects have to be considered when optimizing the composition for the synthesis of the sorbent with overall best functionality.

T a b l e 2 – *Mass loss during the regeneration in TGA apparatus and calculated conversions*

Sample	Mass loss / %	Conversion / %
ZAT 1	3.97	24.08
ZAT 2	3.81	23.10
ZAT 3	4.11	24.92
ZAT 4	5.59	33.90
ZAT 5	3.95	23.95

Conclusions

The novel zinc oxide based sorbents for high temperature gas desulfurization (HTGD) were prepared by sol-gel synthesis. FTIR analysis confirmed optimal synthesis parameters. When thermally

treated at 500 °C samples yield several crystal phases: gahnite, zinc titanate, zinc alumotitanate, zincite and brookite, and show high specific surface areas.

A novel batch reactor for sulphidization of prepared sorbents was introduced. Monitoring of the ZnO–ZnS–ZnO cycle was enabled, revealing the efficiency of prepared sorbents. Sorbent with composition $Zn_{1.75}Al_{0.5}Ti_{0.75}O_4$ was found to possess the highest sulphidation reactivity, i.e. sulphur removal efficiency.

ACKNOWLEDGEMENT

The financial support of the Ministry of Science, Education and Sports of Republic of Croatia within the framework of the project No. 125-1252970-2981 "Ceramic nanocomposites obtained by sol-gel process" is gratefully acknowledged.

Symbols

ν_{as} – asymmetrical stretching mode
ν_s – symmetrical stretching mode
δ_{as} – asymmetrical bending vibration
δ_s – symmetrical bending vibration
Δm_{max} – theoretical mass loss, %
Δm_{reg} – registered mass loss, %
M – molar mass, g mol^{-1}
S_{BET} – specific surface area (obtained by a BET N_2 gas adsorption-desorption isotherm)

Abbreviations

Asb – aluminum sec butoxide
ATR – attenuated total reflectance
BET – Brunauer–Emmet–Teller (N_2 gas adsorption-desorption isotherm)
CPS – counts per second
DTA – differential thermal analysis
DTGA – differential thermo-gravimetric analysis
Eaa – ethyl acetoacetate
FTIR – Fourier transform infrared spectroscopy
HTGD – high temperature gas desulfurization
IGCC – integrated gasification combined cycle
TGA – thermo-gravimetric analysis
Tnb – titanium n-butoxide
XRD – X-ray diffraction
ZAT – zinc alumotitanate sample

References

1. *Kyotani T., Kawashima H., Tomita A., Palmer A., Furimsky E.,* Fuel **68** (1989) 74.
2. *Gangwal S., Turk B., Portzer J., Gupta R., Toy L., Steele R., Kamarthi R., Leiniger T.,* Development of a gas cleanup process for Chevron Texaco Quench gasifier syngas, in *Morsi B. I.* (Ed.), 20th Annual International Pittsburgh Coal Conference – Proceedings, Pittsburgh Coal Conference, Pittsburgh, 2003.
3. *Slimane R. B., Lau F. S., Berry D. A., Carty R. H.,* Development progress on GTI's regenerable zinc titanate sulfur sorbent for fluidized-beds and transport reactors, in *Morsi B. I.* (Ed.), 20th Annual International Pittsburgh Coal Conference – Proceedings, Pittsburgh Coal Conference, Pittsburgh, 2003.
4. *Kobayashi M., Nunokawa M., Shirai H*., Development of regenerable desulfurization sorbent for coal gas sulfur removal below ppm level, in *Schmidt E., Gang P., Pilz T., Dittler A.* (Eds.), High Temperature Gas Cleaning, pp. 618–629, G. Braun Printconsult Gmbh, Karlsruhe, 1996.
5. *Kobayashi M., Shirai H., Nunokawa M.,* Energ. Fuel. **11** (1997) 887.
6. *Jung S. Y., Lee S. J., Park J. J., Lee S. C., Jun H. K., Lee T. J., Ryu C. K., Kim J. C.,* Sep. Purif. Technol. **63** (2008) 297.
7. *McMullan J., Williams, B.,* CLA-98-050641, EDB-98-057390, ETSU-COAL-R-139, IEACR Lib ETSU (1998).
8. *Xu H. Y., Liang M. S., Li C. H., Wang Y. G.,* Journal of Fuel Chemistry and Technology, **33** (2005) 12.
9. *Mojtahedi W., Abbasian J.,* Energy Fuels **9** (1995) 429.
10. *Dancila M., Untea I., Badilita V.,* Rev. Chim.-Bucharest **58** (2007) 640.
11. *Untea I., Dancila M., Vasile E., Belcu M.,* Pow. Teh. **191** (2009) 27.
12. *Christoforou S. C., Efthimiadis E. A., Vasalos I. A.,* Ind. Eng. Chem. Res. **34** (1995) 83.
13. *Garcia E., Cilleruelo C., Ibarra J., Pineda M., Palacios J. M.,* Ind. Eng. Chem. Res. **36** (1997) 846.
14. *Li Y., Guo H., Li C., Zhang S.,* Ind. Eng. Chem. Res. **36** (1997) 3982.
15. *Woods M. C., Gangwal S. K., Jothimurugesan K., Harrison D. P.,* Ind. Eng. Chem. Res. **29** (1990) 1160.
16. *Slimane R. B., Abbasian J.,* Adv. Environ. Res. **4** (2000) 147.
17. *Kurajica S., Mali G., Gazivoda T., Šipušić J., Mandić V.,* J. Sol-Gel Sci. Techn. **50** (2009) 158.
18. *Haridas M. M., Goyal N., Bellare J. R.,* Ceram. Int. **24** (1998) 415.
19. *Silverstein R. M., Webster F. X.,* Spectrometric Identification of Organic Compounds, 6th Ed., J. Willey & Sons Inc, New York, 1998.
20. *Preudhomme J., Tarte P.,* Spectrochim. Acta A. **27** (1971) 961.
21. *Padmaja P., Anilkumar G. M., Mukundan P., Aruldhas G., Warrier K. G. K.,* Int. J. Inorg. Mater. **3** (2001) 693.
22. *Kurajica S., Mandić V., Šipušić J.,* J. Cer. Sci. Tech. **2** (2011) 15.
23. *Konttinen J. T., Zevenhoven C. A. P., Yrjas K. P., Hupa M. M.,* Ind. Eng. Chem. Res., **36** (1997) 5432.
24. *El-Hakam S. A.,* Colloid Surface A. **157** (1999) 157.
25. *Youssef A. M., El-Sharkawy E. A.,* Mater. Lett. **12** (1995) 335.
26. *Bakker W. J. W., Kapteijn F., Moulijn J. A.,* Chem. Eng. J. **96** (2003) 223.
27. *Jung S. Y., Lee S. J., Lee T. J., Ryu C. K., Kim J. C.,* Catal. Today **111** (2006) 217.
28. *Bu X., Ying Y., Zhang C., Peng W.,* Powder Technol. **180** (2008) 253.